Biophysical Chemistry 20 (1984) 135–148
Elsevier

BPC 00871

BUFFER CATALYSIS OF AMINO PROTON EXCHANGE IN COMPOUNDS OF ADENOSINE, CYTIDINE AND THEIR ENDOCYCLIC *N*-METHYLATED DERIVATIVES

Bruce McCONNELL and Diane POLITOWSKI

Department of Biochemistry and Biophysics, John A. Burns School of Medicine, University of Hawaii, Honolulu, HI 96822, U.S.A.

Received 19th September 1983
Revised manuscript received 24th February 1984
Accepted 2nd March 1984

Key words: Proton exchange; Catalysis; NMR line shape; Kinetics; Amino proton; Nucleobase dissociation

The use of buffer catalysts having a wide range of pK' (dissociation) values (4–12) provides the first estimates of two generally useful empirical parameters of amino proton exchange in compounds of adenine and cytosine. These are a nucleobase amino group dissociation constant (pK'_{11}) and the 'encounter frequency' for proton transfer (k_{11}), which can be used to predict amino proton exchange rates. Values of amino pK'_{11} fall in the range 8.6–9.4 for the unsubstituted nucleobases and their endocyclic *N*-methylated derivatives. Similar values of k_{11} are obtained for all nucleobases (1×10^8 M^{-1} s^{-1}). These constants were obtained from a statistical fit of second-order catalytic rate constants for amino proton exchange, measured by amino ^{1}H-NMR lineshape at varying field frequencies (100, 300 and 360 MHz). These results confirm the requirement for buffer conjugate base formation and nucleobase protonation, but point to a different mechanism of exchange at low pH; most probably direct amino protonation for adenine, but not for cytosine compounds. Anionic buffer conjugate bases (phosphate and acetate) show a greater catalytic effect than neutral (nitrogen) bases, especially with cytosine compounds. The use of high concentrations of sodium perchlorate to sharpen amino ^{1}H resonances of 1-methyladenosine is examined, with respect to chemical and rotational exchange and NMR line broadening.

1. Introduction

The importance of gathering fundamental information on the properties of nucleobase exchangeable protons is derived not only from their crucial function as recognition sites in base-pairing, but more recently from their role as sensitive NMR probes of secondary and tertiary structure of DNA and tRNA [1–3]. Because the macromolecule sequesters from solvent the hydrogen-bonded protons of the base-pairs, structural fluctuations control the solvent exchange of these protons. If the intrinsic lifetimes of these protons can be estimated and predictably manipulated, then rates and equilibrium constants for structural mobility of the macromolecule can be extracted from the data [4]. The manipulation of the intrinsic exchange rates is done through the addition of buffer catalysts and is necessary in order to establish the formal kinetic domain that operates under the conditions of the experiment [5].

It is a fortunate circumstance that the exchangeable protons most accessible to the study of oligonucleotides by NMR, the imino protons of the guanine (N-1) and thymine (uracil) (N-3) bases,

Abbreviations: Ampso, 3-[*N*-(α,α-dimethylhydroxyethyl)]amino-2-hydroxypropanesulfonic acid; Hepes, *N*-2-hydroxyethylpiperazine-*N'*-2-ethanesulfonic acid; Mes, α-(*N*-morpholino)ethanesulfonic acid; Mopso, 3-(*N*-morpholino)-2-hydroxypropanesulfonic acid; ^{1}m-Ado, 1-methyladenosine; 2',3'-cAMP, 2',3'-cyclic adenosine monophosphate; ^{5}m-Cyd, 5-methylcytidine; ^{3}m-Cyd, 3-methylcytidine. Protonated forms of the unsubstituted nucleobases are written as ^{1}H-Ado or ^{1}H-Cyd.

are also simplest for the calculation of intrinsic exchange rates. Because these groups are 'normal' acids (having measurable pK values in aqueous solution) the lifetime of the dissociable proton is a straightforward function of the pK of the donor group and the pK of the acceptor (buffer) [6]. Evidence that the equally important amino protons can be studied by NMR of oligonucleotides raises the possibility that their dissociation kinetics may be used in a way similar to that of the imino protons in studying nucleic acid structure [7,8].

The exchange mechanism of the nucleobase amino protons is more complex than that of the imino protons. On the basis of the hydrogen-exchange properties of helical DNA, nucleobase endocyclic protonation was postulated as a necessary prelude to amino proton exchange [9]. Studies at the monomer level showed that protonation of an endocyclic nucleobase site is a requirement for the observation of amino proton exchange at neutral or acidic pH [10,11]. Otherwise, the amino acidity of the nucleobase is too weak to provide measurable exchange. Amino exchange in the neutral nucleobase is catalyzed only by OH^- and at rates much lower than those of the imino functional groups [12]. Even the addition of buffer exchange catalysts results in exchange rates that conform to the kinetic characteristics of a protonated nucleobase intermediate in both monomeric and polymeric systems [9–11,13]. The important parameters of general use in the prediction of exchange rates would be the donor-acceptor encounter rate constant and the dissociation pK value of the amino group of the donor species. Crude estimates of the dissociation pK values of the adenine amino, pK = 7.5–11 and pK ≅ 19 for the protonated and unprotonated species, respectively, are derived from the conformance of these values to kinetic data obtained from a few buffers representing a limited buffer pK range (pK ≈ 6 to ≈ 8) [10,11,13]. Moreover, these estimates depend upon general assumptions of exchange mechanisms which include unconfirmed estimates of the rate constant for the rate of encounter between donors and acceptors as solutes in aqueous solution. In principle, the collection of catalytic data on amino proton exchange for a large range of buffer pK values flanking the magnitude of the amino donor pK should provide a measure of the encounter rate constant as well as the dissociation pK of the amino of the nucleobase donor [6].

We report here catalyst data on adenine, cytosine and their endocyclic N-methylated forms, which represent analogs of the N-protonated intermediates in amino proton exchange. High salt effects employed to aid measurements of 100 MHz line widths in 1-methyladenosine were examined in relation to chemical and rotational exchange. Second-order rate constants of several structurally diverse buffer catalysts in the pK range 4–12 conform sufficiently well to 'Eigen plots' to provide generalized kinetic constants useful for the prediction of nucleobase amino proton exchange for any buffer systems. These constants are an empirical 'encounter' rate constant of $(1-6)\times 10^8$ M^{-1} s^{-1} and an amino pK value of 8.5–9.4, corresponding to the N-protonated or N-methylated nucleobase exchange intermediate. The disagreement between these amino pK values and those determined previously are discussed in relation to the possibility of a direct amino protonation mechanism exclusive to purines.

2. Materials and methods

2′,3′-cAMP, adenosine, ^{1}m-Ado, ^{5}m-Cyd, ^{3}m-Cyd methosulfate, methyl iodide and N,N-dimethylacetamide (Sigma) were used as supplied, as were the buffers, Hepes, Mopso and Ampso (Research Organics, Inc.). Imidazole and 2-methylimidazole (Sigma) were recrystallized from benzene. The synthesis of ^{1}m-Ado was carried out as follows [14]: 5 g adenosine, 5 ml methyl iodide and 65 ml N,N-dimethylacetamide were stirred at room temperature for 22 h and for an additional 20 min after the addition of celite. The filtrate of this suspension was added to 400 ml acetone (Baker, reagent grade) and placed in the cold for 24 h. The light-yellow precipitate was collected by filtration, washed five times with cold acetone and dried in a desiccator. ^{1}H-NMR line widths and chemical shifts of the synthesized and commercial samples in aqueous solution were identical. In order to synthesize ^{3}m-Cyd [15], 3 ml of fresh dry dimethyl sulfate was used to achieve dissolution of 1 g

cytidine dispersed in 5 ml dimethylformamide. After $\frac{1}{2}$ h stirring at 37 °C the mixture was diluted with 13 ml methyl alcohol and brought to turbidity with 85 ml ethyl acetate. Rapid crystallization in the cold produced a 79% yield of compound melting at 230 °C with decomposition and showing no trace of cytidine precursor by pH titration or NMR.

^{1}H-NMR spectra were obtained in CW mode from the Varian HA-100 NMR spectrometer of the Department of Chemistry, University of Hawaii. All spectra for the cytidine compounds, as well as additional spectra on the adenine systems, were obtained from the Nicolet 300 MHz NMR spectrometer in the Department of Chemistry, University of Hawaii and spectra at 360 MHz were obtained from the Bruker HXS-360 NMR spectrometer of the Stanford Magnetic Resonance Laboratory, Stanford University. All high-field NMR experiments were done with the use of Redfield pulse sequence for minimizing the H_2O signal in FT (quadrature) acquisition [16]. Solution pH was measured by a Beckman Model 4500 pH meter and an Ingold combined electrode designed for pH measurement in 5-mm NMR tubes. In most buffer experiments involving 2',3'-cAMP and ^{5}m-Cyd, the pH was adjusted to a value midway between the endocyclic dissociation and buffer dissociation pK values to obtain maximum line broadening [10] and included measurements at a minimum of two additional pH values to confirm the expected pH profile for buffer catalysis (see below). All buffer catalytic rate constants involved measurements at three or more buffer concentrations. Listed buffer pK values (table 1) that differ from literature values were obtained by pH titration in the presence of nucleoside under the solvent conditions employed.

3. Kinetics

These measurements of buffer catalytic rate constants in amino proton exchange depend upon the measurement of amino ^{1}H-NMR line broadening that occurs upon the addition of catalyst [10,11]. The NMR line broadening W_B is established by a slow NMR exchange time scale involving two exchange sites, amino and water, and $\pi W_B = 1/\tau$, a reciprocal lifetime (first-order rate constant comprised of the sum of the separate site reciprocal lifetimes ($1/\tau_{\text{-NH}_2} + 1/\tau_{\text{H}_2\text{O}}$). However, only the forward rate constant $1/\tau_{\text{-NH}_2}$ is measured [12], owing to the large molar excess of water and the relation $P_{\text{-NH}_2}/\tau_{\text{NH}_2} = P_{\text{H}_2\text{O}}/\tau_{\text{H}_2\text{O}}$ where $P_{\text{-NH}_2}$ is the number of moles of all rapidly equilibrating nucleobase species taken together and $P_{\text{H}_2\text{O}} + P_{\text{-NH}_2} = 1$, i.e., $1/\tau = 1/\tau_{\text{-NH}_2} \gg 1/\tau_{\text{H}_2\text{O}}$. The observed buffer-catalyzed rate is described for the total pH range by

$$k_{obs} = \pi W_B = P k_B[B] \tag{1}$$

where k_{obs} (in s^{-1}) is the first-order buffer increment in observed rate, W_B the increase in line width resulting from catalyst addition at a given pH, $\pi = 3.14$, P the mole fraction of the kinetically predominant species of nucleobase, k_B the second-order rate constant for buffer catalysis and B the conjugate base of the buffer, calculated at pH from the uncorrected Henderson-Hasselbalch relation. That the catalytic role of buffer is limited to its function as proton acceptor only is based on previous evidence derived from pH profiles of buffer catalysis and linear buffer concentration effects for both adenine and cytosine nucleotides [10,11]. $P = 1$ (eq. 1) for nucleobases methylated at the endocyclic protonation sites, i.e., Cyd(N-3) and Ado(N-1). However, the unmodified system comprises an equilibrium between the protonated and unprotonated form of the nucleobase. The predominant kinetic species is the protonated form and $P = a_{H^+}/(K_N + a_{H^+})$, where a_{H^+} is the H^+ activity measured by the pH meter and K_N the acid dissociation constant of the nucleobase protonation site [10,11],

$$\pi W_B = \frac{a_{H^+}}{k_N + a_{H^+}} \cdot k_B[B] \tag{2}$$

In this case eq. 2 defines the optimum experimental pH as a value midway between the acid dissociation constants of the nucleobase (pK_N) and buffer (pK_B). This treatment, based on the kinetic predominance of the protonated nucleobase, NH^+ (and the insignificance of the neutral, unprotonated form, N), is derived from the observation that fitted values of K_B obtained at low

pH (where $P_{NH^-} > P_N$) provide an excellent quantitative fit of k_{obs} at all higher pH values (where $P_{NH^-} \ll P_N$). The existence of a pH maximum for exchange broadening in the protonated nucleobase also establishes the fitting of the catalytic rate constants to Eigen plots, and without this pH specification (as would be the case for the neutral nucleobase) the data do not conform to these plots.

Eigen plots [6,17,18] are based on the relation,

$$k_B = \frac{k_D}{1 + 10^{pK_D - pK_B}} \qquad (3)$$

where k_D represents the encounter rate constant for the formation of a donor-acceptor complex for proton transfer and pK_D is the acid dissociation pK of the amino of NH^+: $-NH_2 \rightleftharpoons -NH^- + H^+$. Both these parameters empirically define fitted plots of $\log_{10} k_B$ and buffer pK (pK_B), where k_D represents k_B in the zero-slope region of the plot ($pK_B > pK_D$) and pK_D is expressed in the unit-slope region ($pK_B < pK_D$).

4. Results

4.1. Buffer catalysis

The determination of k_D and pK_D as general kinetic parameters for amino proton exchange (eq. 3) depends on the determination of second-order rate constants, which involves the division of experimental measurements by very small numbers that represent the concentration of buffer conjugate base at pH values far removed from the buffer pK (pK_B). Thus, a small line broadening marginally outside experimental error can lead to a large, chiefly artificial value of k_B (eqs. 1 and 2) that conforms to eq. 3. To establish the reality of the second-order rate constant buffers were added at sufficiently high and varied concentration to produce pronounced line broadening and to demonstrate linear concentration effects. Examples are seen in fig. 1 showing the linear dependence of line broadening with buffer concentration for adenine (as 2',3'-cAMP) and in fig. 2, which shows the logarithmic pH dependence of broadening for ^{1}m-Ado in the presence of buffer as a reflection of the increase in buffer conjugate base. Both figures lend further support to the exclusive catalytic role of the buffer conjugate base used as the basis for this kinetic analysis. An additional criterion for establishing the observation of buffer catalysis is

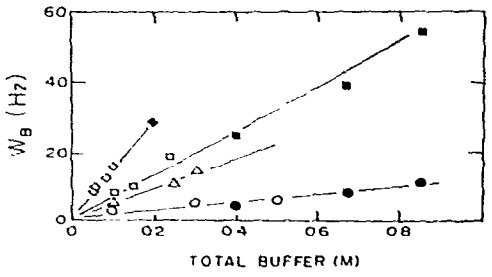

Fig. 1. 2',3'-cAMP amino ^{1}H-NMR line broadening vs. buffer concentration. Spectra were obtained at 26 °C from solutions containing 0.1 M nucleotide and phosphate (◇), tris (□), borate (△), and Ampso (○). Slopes of lines are fitted by eye and reflect solution pH, as well as catalytic rate constants (see text). (◆, ■, ●) Taken at 300 or 360 MHz; (◇, □, △, ○) 100 MHz.

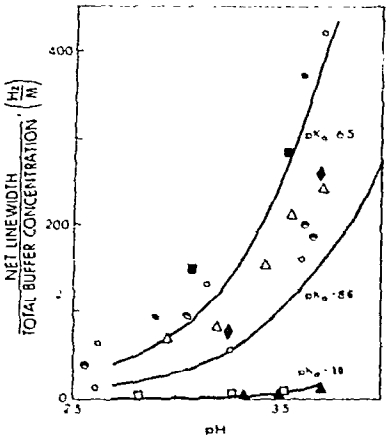

Fig. 2. Specific buffer catalytic line broadening vs. pH for ^{1}m-Ado amino ^{1}H resonances. 100 MHz spectral line widths were obtained at 26 °C after sequential pH adjustments on solutions containing 2.5 M $NaClO_4$, 0.1 M ^{1}m-Ado and the following 0.1 M buffers: acetate (◇), cacodylate (△), phosphate (○), imidazole (●), Hepes (■), Tris (◓), borate (□) and Ampso (▲). Three solid curves are calculated from eq. 3; $k_D = 1 \times 10^8$ M^{-1} s^{-1}, $pK_D = 8.6$ for three conditions; $pK_B = 10 > pK_D$, $pK_B = 8.6 = pK_D$ and $pK_B = 6.5 < pK_D$. The ordinate parameter represent the change in line width, divided by the total buffer concentration.

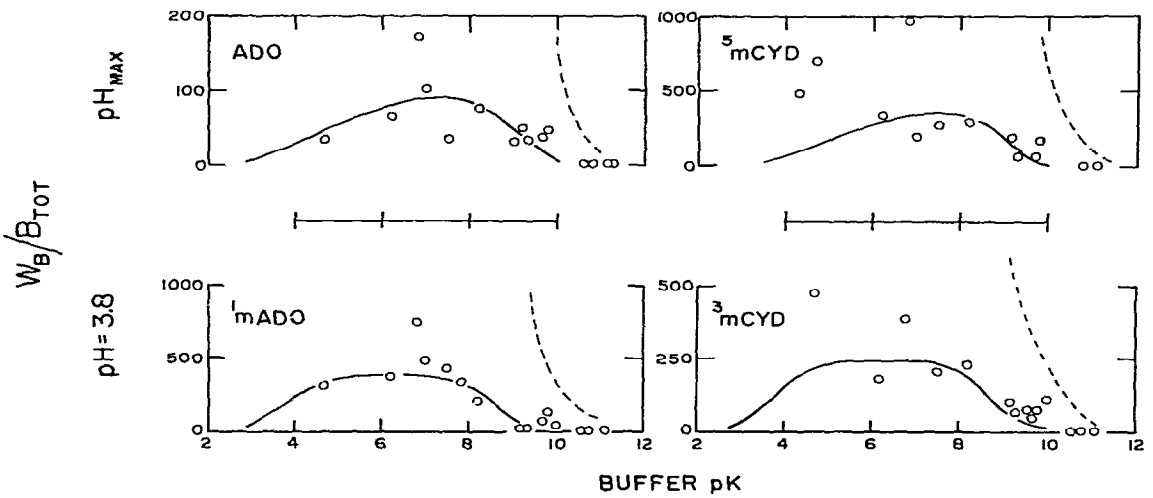

Fig. 3. Specific catalytic broadening as a function of buffer pK. The observed amino ^{1}H-NMR line broadening, divided by the total buffer concentrations is shown (top) for the 'unmodified' nucleobases (as 2',3'-cAMP and ^{5}m-Cyd) corrected to the pH condition of maximum broadening ($0.5pK_N + 0.5pK_B$) and (bottom) for the N-methylated nucleobases (^{1}m-Ado and ^{3}m-Cyd), all measured at pH = 3.8. Solid curves are calculated from eqs. 1–3, with k_D and pK_D values shown in table 2. Dashed curves represent the same calculation with $k_D = 10^9$, instead of 10^8 M^{-1} s^{-1}.

the demonstration that the specific broadening (line broadening divided by total buffer concentration) should vanish at high pK_B values in accordance with eqs. 1–3. This criterion of convergence to low experimental and calculated values at high pK_B is fulfilled (fig. 3), which further shows that a k_D (eq. 3) of 6×10^7 to 6×10^8 provides coincidence, while $k_D = 10^9$ clearly does not in this region. This places $k_D = 6 \times 10^8$ as the upper limit of the encounter rate constant for all of the nucleobase-buffer interactions leading to exchange. In addition, it can be seen from the plots of fig. 3 that the phosphate data for all nucleobases (and those of acetate, as well, for cytidine compounds) show high (≈ 2-fold) positive deviations from the rest of the experimental and calculated values. Accordingly, these two buffers were segregated into a separate class (as anionic bases) from the others (nitrogen, neutral bases) in selecting the global constants, k_D and pK_D for the calculated lines fitting the lower data points (see section 5). These global constants do not differ significantly from their first approximations, obtained by regression analysis of Eigen plots (fig. 6, tables 1 and 2) in which all buffers were weighted equally (see below).

Fig. 3 provides confirmation of the double requirement for (1) the protonated nucleobase and (2) the buffer conjugate base as the important exchange species. Implicit in this confirmation is the necessity for careful selection of pH values represented by the data. Data for the unsubstituted nucleobases represent the pH of maximum buffer catalysis, which lies midway between the pK of the nucleobase endocyclic nitrogen and that of the buffer, as described in section 3. For the methylated nucleobases, the data were collected at pH 3.8, which represents the highest pH where minimum line broadening can be measured in the absence of buffer. The basis for this pH selection is exemplified in plots of NMR line width vs. pH for ^{3}m-Cyd (fig. 4) and ^{5}m-Cyd (fig. 5) reported here for the first time. The 5-methylated compound represents the unsubstituted protonation site system and provides the advantage of accurate line width determinations from a rotationally

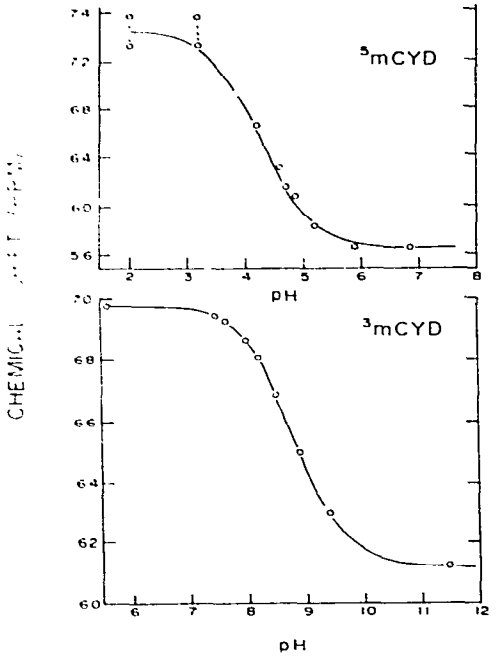

Fig. 4. Chemical shift vs. pH for ^{5}m-Cyd and ^{3}m-Cyd. Chemical shifts were measured relative to an external tetramethylsilane capillary providing a reference signal 3.66 ppm upfield of the water proton resonance for 0.05 M solutions of ^{5}m-Cyd (amino ^{1}H resonance) (top) and ^{3}m-Cyd (H-6) resonance (bottom). Points joined by broken lines below pH 3.5 in the ^{5}m-Cyd titration represent separation of the amino proton resonances as the N-3 site is protonated.

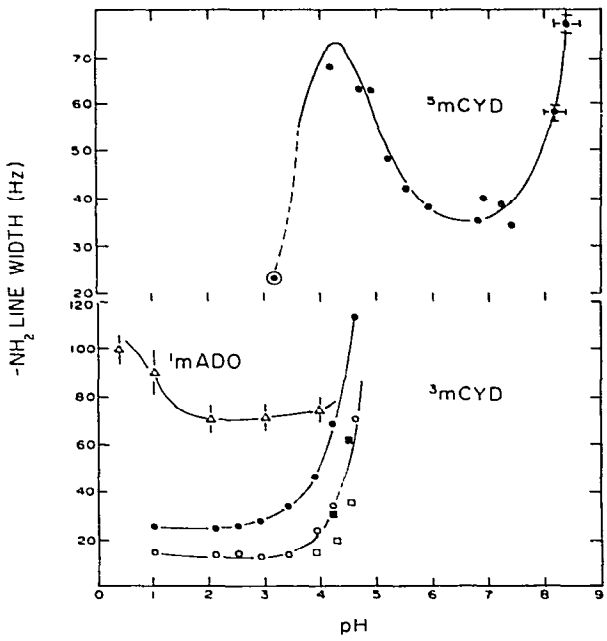

Fig. 5. Observed amino ^{1}H-NMR line width vs. pH for ^{5}m-Cyd, ^{1}m-Cyd and ^{1}m-Ado. (Top) Line width of the amino ^{1}H resonance of ^{5}m-Cyd at 26 °C, 0.05 M nucleoside. Solid line through the data is line broadening calculated from eq. 1, in which B is the conjugate base of the ^{5}m-Cyd N-3 functional group; $k_B = 4.4 \times 10^3$ M^{-1} s^{-1}. These values are added to the minimum line width = 35 Hz. The overstruck point at pH 3.5 represents the equal line width of the separate $-NH_2$ resonances that become resolved below pH = 4. (Bottom) 300 MHz line widths of the ^{1}m-Ado amino ^{1}H resonance obtained at 26 °C, 0.1 M nucleoside (△); 300 MHz line width of the upfield (●) and downfield (○) amino ^{1}H resonances of 0.1 M ^{3}m-Cyd, 26 °C; corresponding values for 0.05 M ^{3}M Cyd (■, □). Solid lines through these data are fitted by eye.

coalesced amino ^{1}H resonance. In cytosine these resonances are separate, grossly broadened and overlapping under the same conditions as a result of slow (C-4)–NH_2 bond rotation [10,19]. Chemical shift-pH titrations of the amino ^{1}H of ^{5}m-Cyd and the (C-6) proton of ^{3}m-Cyd (fig. 4) are fitted with pK values of 4.3 (N-3) and 8.8 (^{3}m-Cyd) $-NH_2$). Line width-pH profiles shown for the amino protons of these two nucleosides establish the selection of the experimental pH for buffer catalysis; pH 3.8 for ^{3}m-Cyd and pH 5.8–7.2 for the minimum line width of the m^5-Cyd amino ^{1}H resonances. For ^{5}m-Cyd the marked broadening in the region pH 3–6 is due to self-catalysis, i.e., the catalytic exchange effect of the (N-3) unprotonated site acting as proton acceptor with a rate constant, $k_B = 4.4 \times 10^3$ M^{-1} s^{-1}. Similar observations have been made with cytosine [10]. The pH profiles for the 1-methyl and substituted adenines have been presented elsewhere [10,20] and are much the same, with the exception that the self-catalysis broadening is not seen in adenine compounds.

Table 1

Experimental and calculated catalytic rate constants of amino proton exchange in *N*-methylated and unsubstituted adenosine and cytosine

Second-order ($M^{-1} s^{-1}$) rate constants, expressed in log form, are based on concentration of buffer conjugate base (not total buffer). Catalyst p*K* values were based on 20–25 °C listings in the Handbook of Chemistry and Physics (CRC), Handbook of Biochemistry and Molecular Biology (Sober, CRC). % Dev., percent deviation of the experimental k_B (not the log) from the value calculated by eq. 3 and the constants of table 2. Exp., experimental; Cal., calculated.

Buffer catalyst	Catalyst p*k*	Adenosine			^{1}m-Ado			^{5}m-Cyd			^{3}m-Cyd		
		Log k_B		% Dev. in k_B	Log k_B		% Dev. in k_B	Log k_B		% Dev. in k_B	Log k_B		% Dev. in k_B
		Exp.	Cal.		Exp.	Cal.		Exp.	Cal.		Exp.	Cal.	
^{5}m-Cyd (N-3)	4.3	–	–	–	–	–	–	3.8	3.4	+151	–	–	–
Acetate	4.7	3.4	3.3	−21	4.3	4.1	+59	4.1	3.8	+100	4.1	3.8	+100
Mes	6.2	4.9	4.9	0	5.5	5.6	−20	5.0	5.3	−50	5.0	5.3	−50
Cacodylate	6.2	4.9	4.9	0	5.5	5.6	−20	–	5.4	–	–	5.3	–
Phosphate	6.8	5.9	5.5	+152	6.3	6.2	+28	6.3	5.9	+153	6.1	5.9	+59
Mopso	7.0	5.3	5.7	−60	6.6	6.4	+63	5.5	6.1	−75	–	–	–
Imidazole	7.0	6.1	5.7	+152	6.6	6.3	+100	–	6.1	–	–	6.0	–
Hepes	7.5	5.8	6.2	−60	6.7	6.9	−32	6.3	6.6	−47	6.4	6.6	−35
2-Methylimidazole	7.8	6.7	6.5	+62	7.2	7.2	0	–	6.8	–	7.0	–	–
Tris	8.2	6.9	6.9	+6	7.2	7.5	−44	6.9	7.2	−50	7.2	7.2	−11
^{3}m-Cyd (-NH_2)	8.8	–	–	–	–	–	–	–	–	–	7.7	7.7	0
Borate	9.2	7.7	7.7	+3	7.2	7.9	−80	7.7	7.8	−12	7.9	7.9	−10
Ampso	9.3	7.3	7.7	−64	7.2	7.9	−81	7.3	7.8	−67	7.6	8.0	−59
Alanine (-NH_2)	9.7	8.0	7.9	+19	8.1	8.0	+36	7.6	7.8	−44	8.1	8.1	0
Glycine (-NH_2)	9.8	8.2	8.0	+76	8.5	8.0	+236	8.2	7.9	+120	8.6	8.1	+201
Phenol	10.0	–	–	–	8.4	8.0	+161	–	–	–	8.7	8.1	+256
Proline (-NH_2)	10.6	–	–	–	8.0	8.0	+1	–	–	–	8.1	8.2	−18
Dimethylamine	10.8	–	–	–	–	–	–	–	–	–	≤ 8.1	8.2	< −19
Ethylamine	10.8	≤ 7.8	8.1	< −49	≤ 8.3	8.0	< 101	≤ 7.8	7.9	−20	≤ 7.9	8.2	< −49
Pyrrolidine	11.1	≤ 8.4	8.1	< 104	≤ 8.7	8.0	< 403	≤ 7.8	7.9	−20	≤ 8.3	8.2	< 27

Listed in table 1 are the experimental rate constants expressed as logs for each of the buffers and their percent deviation from a rate constant calculated from the fitted global parameters, k_D and pK_D, listed in table 2. These parameters were determined by selecting a mean value of k_D from the maximum experimental values of k_B for each nucleobase and applying them with trial values of pK_D to eq. 3 to obtain minimum statistical variance between the calculated and all the experimental points. The alternative procedure of linear regression [22] provided quite similar values of pK_D and k_D, which are listed in parentheses in table 2. In this case, log k_D was determined as the least-squares intercept and the regression slope at minimum variance was 1.0 in all cases. The linear form of eq. 3 was used, in which the dependent variable, $y = \log k_B$ and the independent variable, $x = -\log(1 + 10^{pK_D - pK_B})$ was determined for trial values of pK_D to obtain minimum statistical variance.

Rate constants for certain high-pK_B buffers are shown as maximum values (table 1), since these buffers produced only marginally detectable broadening at high concentrations. Elimination of these values and reduction of statistical weights of all $k_B \approx 10^8$ values produced no change in the regression values of k_D, pK_D and slope. These parameters and their variance for lower trial values of pK_D for adenosine and ^{5}m-Cyd are included in table 2 to show the poor fit associated with these values (see below).

Plots of the experimental and calculated data of table 1 as a function of pK_B (Eigen plots) are shown in fig. 6 for all the nucleobases, in order to exhibit the comparison of all nucleobase compounds in terms of eqs. 1–3. There is little difference in these plots for any of the nucleobases, as seen by the similarity of the k_D and pK_D constants listed in table 2. The pK_D values are known quantities for the endocyclic *N*-methylated nucleobases, which have been determined from chemical shift titrations to be 8.4 and 8.8 for ^{1}m-Ado and ^{3}m-Cyd, respectively (see fig. 5 and refs. 20 and 21). The buffer-derived values are somewhat higher, but their relative magnitudes are maintained which represents good agreement, in view of the diversity of the buffers. The Eigen plots of the *N*-unsubstituted nucleobases represent their endocyclic protonated forms (^{1}H-Ado or ^{3}H-Cyd), which clearly conform to eq. 3 with respect to the $(pK_D - pK_B)$ term. The pK_D values of these species are unknown and not accessible for measurement by pH titration, while the pK_D values obtained here from the buffer data are equal to or even higher than those of the *N*-substituted compounds. These plots show that trial values of pK_D lower than those derived statistically from the buffer data produce extremely large deviations from the experimental values (dashed lines). The lower trial values were based on previous alternative methods for their estimates, based on water (H_2O) as acceptor [10,13] (see below).

As shown in table 2, differences in pK_D be-

Table 2

Amino proton exchange rate constants, Eigen constants and their statistical fit for *N*-methyl- and unsubstituted adenosine and cytidine

Adenosine was determined as the 2′,3′-cyclic phosphate form. Values of k_{HO^-} and k_{H_2O} were taken from refs. 10 and 12. All constants were derived from rates measured at 25 ± 2 °C.

Nucleoside	pK_N	k_{OH} ($M^{-1}s^{-1}$)	k_{H_2O} ($M^{-1}s^{-1}$)	Log k_D	pK_D	Regression slope	Variance	Line fit
Adenosine	3.7	4×10^7	6	8.1 (8.1 ± 0.1) [a]	9.4 (.4)	(1.0 ± 0.1)	0.1	0.98
^{1}m-Ado	–	10^{10}–10^{11}	~1	8.0 (8.0 ± 0.1)	8.6 (8.5)	(1.0 ± 0.1)	0.2	0.95
^{5}m-Cyd	4.3	6×10^7	0.2	7.9 (7.7 ± 0.1)	8.8 (8.8)	(1.0 ± 0.1)	0.1	0.98
^{3}m-Cyd	–	10^{10}–10^{11}	< 0.1	8.2 (8.1 ± 0.1)	9.1 (9.0)	(1.0 ± 0.1)	0.1	0.98
Adenosine	3.7	4×10^7	6	8.0 (7.4 ± 0.2)	7.5 [b]	1.6 ± 0.2	1.9	0.90
^{5}m-Cyd	4.3	6×10^7	0.2	8.0 (7.4 ± 0.1)	7.9 [b]	1.2 ± 0.1	0.75	0.94

[a] Values in parentheses are least-squares constants for the relation, $\log k_B = \log K_D - \log(1 + 10^{pK_D - pK_B})$.

[b] Trial values of pK_D taken from alternative methods (see text).

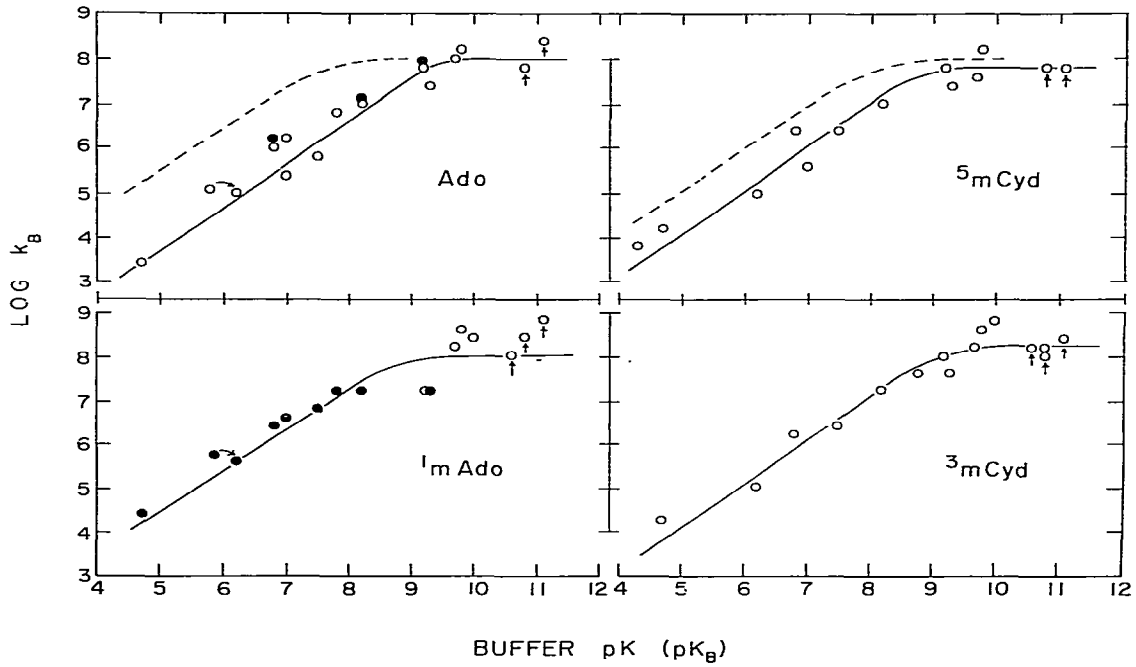

Fig. 6. Log catalytic rate constant as a function of buffer pK_1. Log k_B values, obtained from eqs. 1 and 2, are plotted as a function of pK_B for 2',3'-cAMP, ^{5}m-Cyd, ^{1}m-Ado and ^{3}m-Cyd. (●) Data collected at 2.5 M $NaClO_4$; (○) no additions other than nucleobase compounds and buffer. All points were obtained from line widths collected at 26 °C and at 100, 300 or 360 MHz. Solid lines are calculated from eq. 3 and the constants, k_D and pK_D listed for each nucleoside in table 2.

tween adenine and cytosine compounds are seen with certainty only for the unmodified systems. These values correspond to the dissociation pK of the amino group of the protonated or N-methylated forms and would indicate a lower acidity for ^{1}H-adenine, even compared to ^{1}m-Ado. For comparative purposes two additional kinetic constants are listed in table 2. The first is the rate constant for hydroxyl-catalyzed exchange from the neutral form of the unmodified nucleobase, which is measured by the amino ^{1}H line broadening observed as the pH is raised above neutrality (fig. 6) [12]. These constants are similar for 2',3'-cAMP and ^{5}m-Cyd (4×10^7 and 6×10^7, respectively). The slightly greater value for the ^{5}m-Cyd amino group is consistent with a higher average value obtained from unmodified cytosine, which reflects the higher acidity associated with one of the resolved amino proton resonances in this compound ($k_{OH} = (1-3) \times 10^8$) [11].

The second constant reflects a much more dramatic difference between the amino groups of adenine and cytidine. This constant, k_{H_2O}, pertains to the endocyclic protonated form, as determined from the observed line broadening at pH < pK_N,

$$\frac{\pi W_B}{55} = k_{H_2O},$$

and is based on the assumption that H_2O is the principal acceptor available under this condition. This constant is at least one order of magnitude greater for adenine, compared to cytosine. It is noteworthy that the use of k_{H_2O} as k_B in eq. 3 for

adenine gives a value of $pK_D = 7.5$ ($k_D = 10^{10}$ and $pK_B = -1.7$). This value is close to the pK_D determined from stopped-flow measurements by other workers ($pK_D = 7.8$) [13], but has been shown above to be clearly at variance with the buffer data. The much lower value for cytosine compounds, $k_{H_2O} = 0.2\ M^{-1}\ s^{-1}$, is based on the small measurement of a few hertz broadening of the amino ^1H resonances between pH 0 and 1. In this case the corresponding amino acidity value of protonated cytosine, $pK_D = 9$, is in much better agreement with the buffer data presented here.

Additional observations can be made from an inspection of table 1 and fig. 6 in regard to deviations for certain buffers. The most notable is the consistently high k_B for phosphate ($pK_B = 6.8$), glycine ($pK_B = 9.8$) and high values for acetate ($pK = 4.7$) in the results on cytidine compounds. Preliminary evidence indicates that the glycine-induced broadening might be nonlinear with buffer concentration. The other amino acids, alanine and proline, produce no similar excess values. Low deviations are observed with borate and Ampso in the case of ^{1}m-Ado, but not for the other bases. In addition, the overall variance of data in the ^{1}m-Ado system was greater than that of the other nucleobases. Therefore, the line broadening factors were examined in more detail for this modified nucleobase, with consideration of the high salt solutions used to facilitate line width measurements.

4.2. Salt effects

Minimum line widths of the amino ^1H resonance of ^{1}m-Ado follow the same pH dependence shown for ^{3}m-Cyd in fig. 5, but are established by a much broader, rotationally coalesced resonance that severely limits the range of accurate measurements of catalytic broadening. From initial studies at 100 MHz it was found that the amino ^1H resonance was dramatically sharpened by the addition of high concentrations of $NaClO_4$ or similar neutral salt, possibly as a result of decreased water available as proton acceptor in these solutions [20]. To explore this possibility as a means for obtaining narrow line widths experiments were carried out to determine the salt effect, to examine line broadening factors other than exchange and

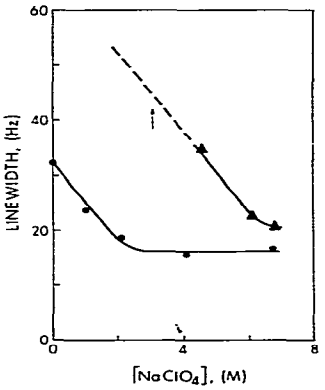

Fig. 7. The effect of $NaClO_4$ on the amino ^1H-NMR line widths of ^{1}m-Ado and adenosine. Solutions contained 0.1 M ^{1}m-Ado at pH 3 (●) and 0.2 M adenosine at pH 2 (▲). Line widths were taken from spectra obtained at 100 MHz and 26 °C. Vertical arrow in dashed portions of adenosine plot represent the minimum value for a severely broadened resonance.

to establish that catalytic broadening is a function of buffer conjugate base in high salt solutions.

As shown in fig. 7, the 100 MHz amino line width of ^{1}m-Ado decreases from 35 Hz to a constant value of about 15 Hz as the $NaClO_4$ concentration is increased to above 2.5 M. That this decrease is due to salt attenuation of the exchange rate is supported by data shown in the figure for unsubstituted adenosine (^1H-Ado) amino line width at pH 2. At this pH, amino exchange of adenosine produces a considerably greater broadening in the slow NMR exchange limit, owing to the greater exchange rate of the protonated species and provides a greater range of exchange rates to be affected by the salt. Accordingly, the line narrowing for ^1H-Ado occurs through a larger range of $NaClO_4$ concentration and reaches its minimum value above 6 M. The 20 Hz sharpening of the ^{1}m-Ado resonance can be taken as the amount of exchange produced by H_2O as acceptor, i.e.,

$$k_B = \frac{\pi \times 20}{55} = 1.1\ m^{-1}\ s^{-1}.$$

If we assume that k_D for direct solvent catalysis is $10^{10}\ M^{-1}\ s^{-1}$ [6] and pK_E for water is -1.7, then

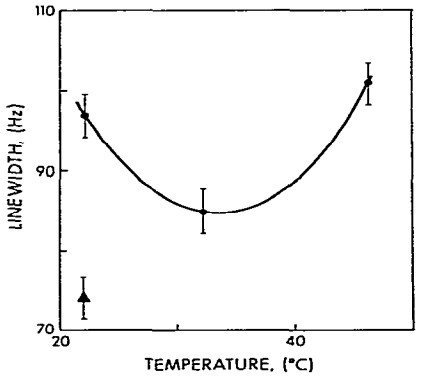

Fig. 8. Effect of temperature on the 360 MHz line width of the ^{1}m-Ado amino ^{1}H resonance. Measurements were taken from 0.1 M nucleoside at pH 3.8 containing 2.2 M $NaClO_4$ (▲) and with no added salt (●).

eq. 3 provides a value of $pK_D = 8.3$, in fairly good agreement with the titration value of 8.4–8.5. However, this agreement would not be seen at lower pH (< 2) (see section 5).

There is a marked NMR frequency dependence of the amino ^{1}H line width for ^{1}m-Ado, which indicates a second major exchange process contributing to line shape in this molecule (fig. 8). At 20 °C, the 35 Hz line width at 100 MHz increases to 76 Hz at 300 MHz and to 97 Hz at 360 MHz. The possibility of intermolecular interaction can be discarded in favor of limited (C-6)–NH_2 bond rotation as the source of this additional line broadening, since the observed line width was unchanged for large changes in nucleobase concentration (not shown). As shown in fig. 8 the marked line sharpening as temperature is increased from 20 to 30 °C reveals that rotation dominates line shape in this temperature range as a 'moderate fast' exchange process proceeding to 'fast exchange' on the NMR time scale and that the broadening between 30 and 40 °C is due to the chemical exchange contribution in the 'slow' exchange region.

$$W_{\mathrm{Obsd}} = \frac{1}{\pi T_2} + \frac{1}{\pi \tau} + W_{\mathrm{F}},$$

where W_{Obsd} the total width, T_2 the transverse relaxation time giving the 'natural' line width, τ the solvent exchange lifetime, W_{F} the rotational contribution and $\pi = 3.14$. The rotational exchange contribution at 100 MHz is estimated to be 5–6 Hz at 26 °C from the relation,

$$W_{\mathrm{Obsd}}(360\ \mathrm{MHz}) = W_{\mathrm{Obsd}}(100\ \mathrm{MHz}) = \left[(3.6)^2 W_{\mathrm{F}}(100\ \mathrm{MHz})\right] - W_{\mathrm{F}}(100\ \mathrm{MHz}),$$

where $W_{\mathrm{F}}(360\ \mathrm{MHz}) = 65$ Hz. It is also apparent that line sharpening by $NaClO_4$ at 360 MHz (24 Hz) is greater than that obtained at 100 MHz (15 Hz). This is to be expected from previous observations that the (constant) rotational rate at a given temperature is shifted to a 'faster' process on the NMR time scale by an unequal salt effect on the chemical shift (δ) that each amino proton would have in the absence of rotation [19]. This decrease in the rotational parameter, $\Delta\delta_r$, would have little effect at 100 MHz within experimental error. Therefore, the 100 MHz line broadening by the addition of buffer in the presence or absence of salt would be a measure of buffer-catalyzed proton exchange for ^{1}m-Ado. On the other hand, it is possible that broadening effects of buffer might originate partly from a change in $\Delta\delta_r$ when measured at higher fields (300–360 MHz) and that these rotation effects may be diminished through the addition of salt.

The demonstration shown in fig. 2 that the buffer conjugate base is the major catalyst for ^{1}m-Ado was carried out in 2.5 M $NaClO_4$ and at 100 MHz. The amino proton resonances, normally unaffected in the pH range shown, broaden logarithmically in the presence of buffers as the pH is increased. The data fall into three domains indicated by the solid lines, which were calculated from eq. 3 for $pK_B = 6.5 < pK_D$, $pK_B = 8.6 \approx pK_D$ and $pK_B = 10 > pK_D$. It is noteworthy that the data on borate ($pK_B = 9.2$) and Ampso ($pK_B = 9.3$) conform to the $pK_B = 10$ calculated values. Similar low values are obtained at 300 and 360 MHz, in both the presence and absence of salt. Therefore specific effects of buffers on line width are not accounted for by changes in $\Delta\delta_r$ and do reflect catalytic activity. Rate constants obtained in the presence of $NaClO_4$ are 2-fold greater than those

derived from salt-free solutions at 360 MHz. This difference appears to be systematic, independent of buffer species and is borne out by comparison of rate constants measured in the 2',3'-cAMP system in the absence and presence of 2.5 M $NaClO_4$ (closed circles in fig. 6).

5. Discussion

In this work second-order rate constants were determined for several buffers differing in ionic charge, number of functional groups, polarity and molecular structure without correction for statistical or ionic effects [23]. In spite of these differences the correlation of these rate constants with buffer pK is remarkably good, producing an overall fit of eq. 3 and demonstrating further the dual requirement for the protonated nucleobase and the buffer conjugate base as the only important exchange species in the pH range between pH 4 and 7. The N-methylated nucleobases are shown to be exchange analogs of the N-protonated form, which further supports the exclusivity of nucleobase protonation and buffer dissociation in the exchange mechanism. The restriction of the amino proton exchange mechanism to the protonated nucleobase and the conjugate buffer base as intermediates is further supported by lines of evidence other than that presented here. In the amino proton exchange of guanosine compounds the inductive effect of nucleobase protonation is small and no buffer catalysis is seen, except for phosphate [24] which shows exceptionally high values here. The competition of a bulky cation such as methyl mercury cation with the proton for the endocyclic ligand site removes the proton's inductive effect and drastically reduces amino proton exchange [25,26]. Finally, it has been shown that the cytosine resonances of self-complementary oligonucleotides can be assigned and isolated experimentally on the basis of the strict requirement for endocyclic protonation in amino proton exchange in the physiological pH range (McConnell, unpublished data). Therefore, the definitions of 'general acid catalysis' and 'general base catalysis' as descriptions involving either the neutral (unprotonated) nucleobase or the buffer conjugate acid as exchange intermediates would misrepresent amino proton exchange of nucleic acids as it occurs in any pH range.

While the plots of fig. 3 provide the least distorted view of the essential character of buffer catalysis data, the Eigen plots of fig. 6 show the conformance of catalysis to eq. 3 and the maximum values attainable for the second-order rate constants, which clearly do not exceed 6×10^8. This analysis provides two kinetic parameters that can now be used with eqs. 1–3 to predict exchange rates for any buffer system or combination added to solutions of nucleobase-containing molecules. These are pK_D, a dissociation pK value for the amino group of the protonated nucleobase and K_D, an encounter rate constant required for the formation of the proton transfer complex formed between amino donor (the protonated nucleobase) and acceptor (buffer conjugate base). It is noteworthy that neither of these empirically determined constants conforms to expected values that are assumed to be valid for the prediction of exchange rates by other workers. First, the k_D value of $(1–6) \times 10^8$ is two orders of magnitude lower than that commonly accepted in such predictions (see, for example, refs. 5, 9 and 10). It is possible that the application of amino proton exchange data to the relationship expressed by eq. 3 does not provide an accurate value of the actual diffusion encounter rate as defined by Eigen and others [6,17,18]. Additional terms in the kinetics could exist as, for example, a pre-equilibrium involving nucleobase protonation that might reduce the frequency of fruitful exchange encounters, effectively reducing the steady-state concentration of protonated nucleotide. However, there are considerations favoring the validity of $k_D \approx 10^8$. Actual measurements published that provide the higher values of 10^{10} are only made for recombination reactions involving solvent species as donor or acceptor, i.e., OH^- or H_3O^+. We are not aware of any solute-solute transfer measurements of this magnitude, unless these reactions were mediated by a solvent bridge in the hydrogen-bonded complex. On the other hand, the lower encounter rates for buffer-catalyzed proton transfer (10^8) account for observed exchange rates for fast nucleobase imino groups of known pK in cases not requiring

nucleobase protonation [11]. It is not unreasonable to expect that the encounter frequency associated with proton transfer between two solutes (as opposed to solute and solvent) could be 10^2 lower than that of direct solvent-mediated exchange. Solute-solute proton transfers would reflect orientational constraints to the formation of the activated complex [17] and must express as well the necessity of breaking solute-solvent hydrogen bonds in order to form the solute-solute bond, which is sin qua non for proton transfer. Second, the amino dissociation pK values (pK_D) of approx. 9 are higher than previous estimates of 7.8 [13] and 7.4 [10] made for this parameter in the case of adenosine compounds. As shown in fig. 6 these lower pK_D values are well outside the error and variance of the experimental measurements. These lower estimates were derived from exchange measurements taken at low pH values where the nucleobase is fully protonated. Accordingly, it was assumed that the donor species was represented exclusively by the neutral amino group of the endocyclic protonated nucleobase, as in buffer catalysis. Since water is the acceptor (in this case), ($k_D = 10^{10}$ and p$K_B = -1.7$), eq. 3 gives pK_D = 7.4 from the observed line broadening [10]. However, there are two observations that place this mechanism in question as a low pH route for exchange: (1) The amino group of cytidine, more acidic than that of adenosine, exhibits very little, if any exchange at low pH, as is expected from extrapolation of the buffer data to a buffer pK value of -1.7, even for an encounter rate of 10^{10}; (2) While neither cytidine nor ^{3}m-Cyd exhibits low pH exchange at low pH, ^{1}m-Ado shows large exchange broadening at pH below pH 3, revealing a mechanism exclusive of nucleobase protonation, such as direct amino protonation. In direct amino protonation the more basic pK_D values for the adenosine compounds compared to the cytidine compounds (table 2) would explain why low-pH exchange is seen in adenosine, but not in cytidine. (3) Low-pH broadening of the amino resonances are seen in guanosine and 7-methylguanosine compounds, which exhibit no catalysis by buffers that are effective in adenosine and cytidine systems [24]. Moreover, direct amino protonation by hydronium ion to form -NH_3^+, followed by amino proton transfer to H_2O would require only 10^{-9} M of the intermediate to account for all of the observed exchange at low pH. Therefore, the assignment previously determined for amino pK values to the amino of ^{1}H-adenine is suspect and we favor the higher pK_D values as more accurate estimates of amino dissociation constants in the protonated nucleobase. Since the effects of nucleobase endocyclic protonation are not large enough in guanosine compounds to allow buffer-catalyzed exchange they are not expected to be profound in the case of adenosine and cytidine, when consideration is given to the magnitude of the amino pK of the unprotonated species. Although this amino basicity in the neutral nucleobase appears superficially to be greater than that of OH^- [12], it is possible that an amino 'pK' for this form is closer to a value of 13 or 14, in view of the restrictions in hydrogen bond formation with OH^- [27] and recent measurements of nucleobase amino pK values [28]. A reduction of amino pK by 4–5 units with endocyclic protonation (14–9) is more reasonable than a 6–7 unit change associated with p$K_D \approx 7$.

Acknowledgements

This research was supported in part by National Science Foundation Grant PCM 77-20154. Experiments on adenine compounds were performed as partial fulfillment of requirements for Master's Degree by D.P. The Bruker HXS 360 NMR spectrometer is a national facility at the Stanford Magnetic Resonance Laboratory, Stanford University, which is supported by NSF Grants GR 23633 and NIH Grant RR 00711. The Nicolet 300 MHz spectrometer was acquired from funds awarded by the National Science Foundation, NSF Grant CHE 81-00240.

References

1 C.W. Hilbers, in: Biological applications of magnetic resonance, ed. R. Schulman (Academic Press, New York, 1980) p. 1.
2 B.R. Reid, Annu. Rev. Biochem. 50 (1982) 969.
3 D.J. Patel, Annu. Rev. Phys. Chem. 29 (1977) 337.

4 D.M. Crothers, P.E. Cole, C.W. Hilbers and R.G. Schulman, J. Mol. Biol. 87 (1974) 63.
5 C.W. Hilbers and D.J. Patel, Biochemistry 14 (1975) 2656.
6 M. Eigen, Angew. Chem. Int. Ed. 1 (1964) 1.
7 D.J. Patel, Biopolymers 16 (1977) 1635.
8 D.J. Patel, Eur. J. Biochem. 83 (1978) 453.
9 H. Teitlebaum and S.W. Englander, J. Mol. Biol. 92 (1975) 55.
10 B. McConnell, Biochemistry 13 (1974) 4516.
11 B. McConnell, Biochemistry 17 (1978) 3168.
12 B. McConnell and P.C. Seawell, Biochemistry 11 (1972) 4382.
13 D.G. Cross, A. Brown and H.F. Fisher, Biochemistry 14 (1975) 2747.
14 J.W. Jones and R.K. Robins, J. Am. Chem. Soc. 85 (1963) 193.
15 P. Brookes and P.D. Lawley, J. Chem. Soc. (1962) 1348.
16 A.G. Redfield, Methods Enzymol. 49 (1978) 253.
17 J.E. Crooks, in: Proton transfer reactions, eds. E.F. Caldin and V. Golds (John Wiley and Sons, New York, 1975) p. 153.
18 E. Grunwald and D. Eustace, in: Proton transfer reactions, eds. E.F. Caldin and V. Golds (John Wiley and Sons, New York, 1975) p. 103.
19 B. McConnell and P.C. Seawell, Biochemistry 12 (1973) 4426.
20 D.L. Hoo and B. McConnell, J. Am. Chem. Soc. 101 (1979) 7470.
21 J.B. Macon and R. Wolfenden, Biochemistry 7 (1968) 3453.
22 P.R. Bevington, Data reduction and error analysis for the physical sciences (McGraw-Hill, New York, 1969) p. 92.
23 D.M. Bishop and K.J. Laidler, J. Chem. Phys. 42 (1965) 1688.
24 B. McConnell, D.J. Rice, F.-D.A. Uchima, Biochemistry 22 (1983) 3033.
25 B. McConnell, J. Am. Chem. Soc. 104 (1982) 1723.
26 B. McConnell and D.L. Hoo, Chem.-Biol. Interactions 39 (1982) 351.
27 A. Margolin and F.A. Long, J. Am. Chem. Soc. 95 (1973) 2757.
28 S.E. Taylor, E. Buncel and A.R. Norris, J. Inorg. Biochem. 15 (1981) 131.